JOURNAL OF RESEARCH of the National Bureau of Standards—C. Engineering and Instrumentation
Vol 67C, No. 2, April–June 1963

Analysis of a Microwave Radiometer for Precise Standardization of Noise Sources

Gray D. Ward* and John M. Richardson

(January 4, 1963)

Calibration of microwave noise sources requires a standard source, an attenuator, and an instrument for comparing microwave power levels. A modified Dicke radiometer is used for this comparison. A detailed analysis of the radiometer is undertaken employing the cascading matrix of each waveguide element, in order to evaluate the balance error. The analysis accounts for the general case of noise power arising from lossy elements of the radiometer and shows how these can often be accounted for by discussing temperatures in excess of some reference temperature T_0. It also displays several potential sources of error in such radiometers and provides the quantitative basis for keeping these sufficiently small. Fluctuations are analyzed as a basis for estimating sensitivity of measurement. Procedures for adjusting the radiometer to account for the characteristics of the two input paths are given. The results are carried through second order in the various reflection coefficients or related scattering matrix elements involved, which are assumed to be small quantities.

1. Introduction

The National Bureau of Standards is concerned with the development and maintenance of national standards of microwave noise power and with calibration of working or interlaboratory standards. This work requires a standard source, a source to be calibrated, an attenuator, and a radiometer for detecting the equality of microwave noise power levels [Dicke, 1946; Selove, 1954; Mayer, McCullough, and Sloanaker, 1958; Estin, Trembath, Wells, and Daywitt, 1960; Wells, Daywitt, and Miller, 1962]. One source is attenuated a known amount until its power level is equal to the power level of the second source. In order to evaluate the calibration, all errors introduced by the radiometer must be known to second order in the small error quantities. No such analysis is found in the literature.

The radiometer is first described. An analysis of the waveguide portion is undertaken using the cascading and scattering matrices of network components. Noise arising in the networks is explicitly included. The mixer-IF is analyzed, and spectra at various points in the receiver are described. The effects of statistical fluctuations are estimated. The analysis yields a balance equation which is specialized to three convenient methods of operation. A typical error analysis is performed with particular scattering matrices. Finally, all errors are evaluated numerically and summarized.

2. Description of Radiometer

One source of microwave noise power is an argon gas discharge tube located within a rectangular waveguide [Mumford, 1949; Johnson and Deremer, 1951; Knol, 1951; Bridges, 1954; Knol, 1957]. The noise power produced by a gas discharge may be calculated if thermodynamic equilibrium is assumed; however, such an assumption is not justified. Such calculated results could be in error by about 0.5 db. The noise power from such a device is stable, however, to better than 0.001 db when the discharge current is regulated. The argon noise source employed for WR 90 waveguide (8.20 Gc/s to 12.4 Gc/s) consists of a tube about 1 cm in diameter and 30 cm long mounted at a small angle to the axis of a rectangular waveguide, intersecting the broad wall of the waveguide.

The most suitable standard of microwave noise power is a blackbody radiator [Sutcliffe, 1956], the power of which is given by the low frequency approximation to the Planck radiation law. One configuration may consist of a uniform piece of sintered silicon carbide mounted in a

*Present address, University of Redlands, Redlands, Calif.

waveguide section, as shown in figure 1, and heated to a uniform temperature of about 1,000 °K. Water cooling is used on one end of a short stainless steel thermal insulating section, so the temperature drop is taken across a short distance (1 cm).

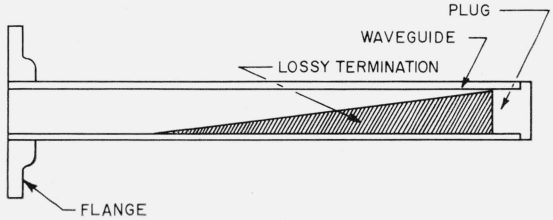

FIGURE 1. *A typical standard may consist of a lossy termination in low-loss waveguide.*
The standard is heated in an oven.

The radiometer is patterned after that of Dicke, with ferrite modulators in place of his rotating vane attenuators (figs. 2a and 2b). In critical applications, motor-driven rotary vane attenuators may serve as modulators, as ferrite modulators may have drifting characteristics and are sensitive to stray magnetic fields. Each input is alternately connected to the hybrid junction, after which the signal from either source travels the same path. The modulated noise signals are heterodyned to an intermediate frequency by a local oscillator and amplified. The signal is further detected, filtered by a narrow-band filter centered at the modulation frequency, amplified, and ultimately displayed on a recording galvanometer.

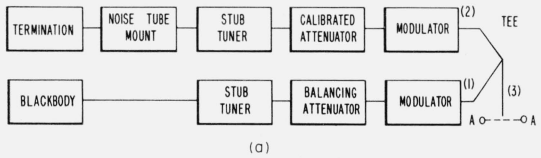

FIGURE 2a. *Generator portion of a radiometer.*

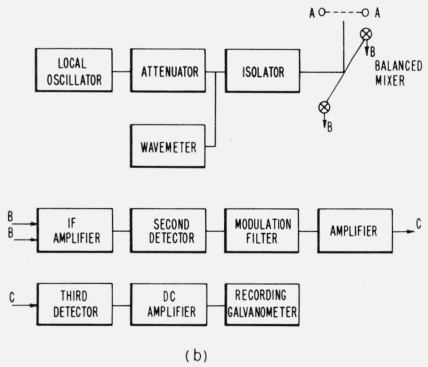

FIGURE 2b. *Receiver portion of radiometer.*

We shall derive an adjustment procedure that compensates many of the inequalities in the two branches of the radiometer. The analysis is done in detail so as to clearly display all the assumptions and approximations that are used. Other waveguide configurations are easily analyzed by the matrix methods presented here.

A calibrated attenuator is used to attenuate the source with higher power until the unknown source and the known source balance each other. The final calibration is in terms of decibels above $kT_0\Delta\nu$ [IRE, 1960], where k is Boltzmann's constant, T_0 is an accepted reference temperature, and $\Delta\nu$ is the limiting RF bandwidth of the system. The maximum resolution of source temperature is limited by system noise and the bandwidths of the system, which determine output fluctuations.

3. Radiometer Analysis—Waveguide Portion

The radiometer waveguide network shown in figure 2a is a member of a general class of waveguide networks which consists of the connection to a common junction of arbitrary groups of series-connected two-port components. Each group may be represented by its equivalent

cascading matrix, which is the product of the cascading matrices characterizing each two-port component. Such a network is shown in figure 3a. We shall be interested in the voltage at reference plane A–A. We shall therefore represent each cascading matrix and source by an equivalent source of reflection coefficient Γ'_i, and equivalent temperature T'_i, as shown in figure 3b. For consideration of the voltage at reference plane A–A, the network to the left of the reference plane may be replaced by an equivalent source of impedance z_G, reflection coefficient Γ_G, and containing an equivalent generator of voltage e_G, as shown in figure 3c.

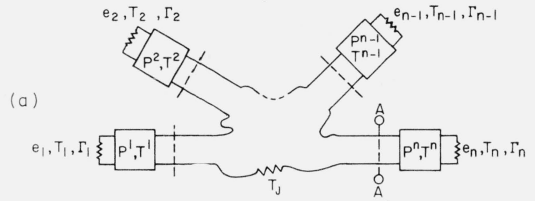

FIGURE 3a. *General* n-*port network with losses, equivalent to figure 2a.*

Each of n arms contains a total equivalent cascading matrix P_i at a temperature T_i. The junction is at a temperature T_J. We shall be concerned with the voltage at reference plane A–A, shown in arm n.

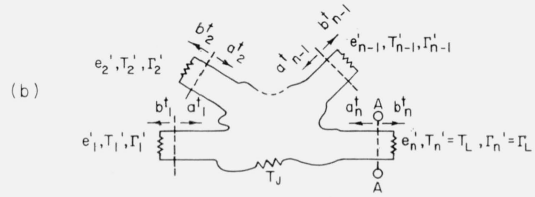

FIGURE 3b. *This general* n-*port network is the one in which the sources and cascading matrices shown in figure 3a have been replaced by equivalent terminations at temperatures* T_i', *source voltages* e_i', *and with reflection coefficients* Γ_i'.

The reference plane A–A is shown.

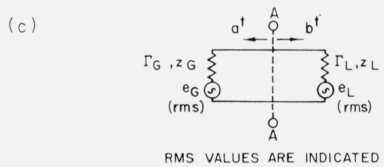

FIGURE 3c. *In this figure, the entire network of figure 3b to the left of reference plane A–A has been replaced by an equivalent generator of voltage* e_G, *with an equivalent source reflection coefficient* Γ_G *which is related to the equivalent generator impedance* z_G.

The waves a^t and b^t are discussed in the text. The direction of these waves is intentionally chosen as shown in order to correspond to the incident and emergent waves at the reference planes A–A in figures 3a and 3b.

In figure 2b the mixer-IF output voltage is postulated to be a linearly related to the voltage at its input terminals. The rest of the receiver may operate further on this voltage to give an output indication related to this voltage, such as the modulation amplitude or its mean square, apart from superimposed statistical fluctuations, of course.

We must calculate the total terminal voltage at reference plane A–A as shown in figure 3. We shall solve for this voltage in figure 3c, then generalize to figure 3b, and finally generalize to figure 3a. This solution may then be used with appropriate simplifications to analyze the particular configuration of figure 2a.

At any kth reference plane of the network, the real, time dependent fields, if restricted to a finite time interval often conveniently normalized to unity, may be represented by a Fourier integral. Provided the interval is sufficiently long, the Fourier amplitudes become known in magnitude in the sense that they have a spectral density (on the axis of frequency ν) relatable to kT. Each Fourier component of the fields of a given mode may, from well-known waveguide theory, be discussed by means of amplitude coefficients v_k, i_k, a_k, and b_k. These coefficients are closely related to voltages, currents, and incident and emergent voltage waves, respectively. These quantities, applicable to a single assumed propagating mode, are related through the characteristic impedance z_0 (here assumed the same for each arm) by the equations

$$v=a+b, \tag{3.1}$$

$$z_0 i=a-b, \tag{3.2}$$

where the subscript k has been dropped.

We may therefore discuss transmission through the network using complex amplitudes of harmonically time dependent voltage density waves at frequency ν and synthesize to the actual case of nonsinusoidal time dependence of noise by the usual integration over the appropriate frequency range. The network transmission properties will be characterized by matrices whose elements are complex functions of ν. The mean square voltages over the time interval or the powers may be obtained by Parseval's theorem, that is, an integration of the square of the absolute value of the (normalized) Fourier amplitude over a frequency range which spans the limiting bandwidth of the system. This relation makes it convenient to deal with rms rather than peak values of a, b, and v in what follows.

The waves a^t and b^t in figure 3c may be decomposed into two parts, given by

$$a^t=a+a^0=\Gamma_L b^t+a^0, \tag{3.3}$$

$$b^t=b+b^0=\Gamma_G a^t+b^0. \tag{3.4}$$

The quantity a^0 or b^0 is the wave that would be launched down a reflectionless line by the particular generator, L or G, respectively. For a^0, a reflectionless line would mean $\Gamma_G=(z_G-z_0)/(z_G+z_0)=0$, or $z_G=z_0$, and similarly for b^0. Then

$$a^0=e_L z_0/(z_0+z_L)=\tfrac{1}{2}(1-\Gamma_L)e_L, \tag{3.5}$$

$$b^0=e_G z_0/(z_0+z_G)=\tfrac{1}{2}(1-\Gamma_G)e_G. \tag{3.6}$$

It may easily be shown, using (3.1), (3.2), and (3.4) that

$$v=a^t+b^t=(1+\Gamma_G)a^0/(1-\Gamma_L\Gamma_G)+(1+\Gamma_L)b^0/(1-\Gamma_L\Gamma_G). \tag{3.7}$$

Γ_G and Γ_L are independent of frequency for sufficiently small $\Delta\nu$. Γ_L is fixed for a particular receiver input impedance, and Γ_G will not vary during the process of making a measurement by adjusting the calibrated attenuator if the radiometer is properly designed. These observations permit us to absorb the coefficients of a^0 and b^0 in (3.7) into the constants of the receiver response and to focus attention on a^0 and b^0 only. To the extent that the equivalent reflection coefficient Γ_G of the source is not constant as the radiometer is operated, an error is incurred. If the variation of Γ_G is known, a correction could be applied. If a^0 is constant also, the receiver output is, apart from a constant, proportional to b^0.

This situation is generalized to the general n-port network of figure 3b. The equivalent source e_G results from that portion of the network to the left of the reference plane A–A in figure 3b. Let there exist at each port of the network an incident wave a^t and an emergent wave b^t. We index the ports by $i=1, 2, \ldots, n$.

Consider the total incident wave a_i^t at port i. By the superposition theorem it consists of the sum of contributions from each source of the network operating alone. We index the sources by $\lambda=0, 1, 2, \ldots, n$, where the index zero designates sources in the junction, and the other indices designate the sources terminating the respective arms. For $\lambda\neq i$, the contribution $a_{i\lambda}$ is that partial wave incident on the ith reference plane which has been established by the source $\lambda\neq i$. This partial wave, incidentally, is a reflection from Γ_i'. For $\lambda=i$, it is convenient to further decompose the partial wave established by the source $\lambda=i$ into parts a_i^0 and a_{ii} where a_i^0 is the wave that would be launched by the source i down a reflectionless line, and a_{ii} is the remainder of the actual partial wave established by the source $\lambda=i$. Only the portion a_{ii} is a reflection from Γ_i'. These considerations may be expressed as

$$a_i^t=a_i^0+\sum_{\lambda=0}^{n}+a_{i\lambda}=a_i^0+a_i. \tag{3.8}$$

The total emergent wave b_i^t at port i likewise consists of the superposition of contributions from all sources in the network. For $\lambda\neq 0$, the contribution $b_{i\lambda}$ is that wave emergent from the ith reference plane which has been established by the source $\lambda\neq 0$. This partial wave,

incidentally, is a scattering of all the incident waves. For $\lambda=0$ it is convenient to decompose the contribution from the sources within the junction into parts b_i^0 and b_{i0}, where b_i^0 is the wave which would be launched by the junction source ($\lambda=0$) down arm i if $\Gamma_i'=0$ for all i, and b_{i0} is the remainder of the actual partial wave established in arm i by the source 0. Only the portion b_{i0} is a scattering of incident waves. Thus the expression

$$b_i^t=b_i^0+\sum_{\lambda=0}^{n} b_{i\lambda}=b_i^0+b_i \tag{3.9}$$

represents the total emergent wave at port i.

The analysis preserves the familiar reflection law for the partial waves in the form

$$a_{i\lambda}=\Gamma_i' b_{i\lambda}, \qquad \lambda\neq 0,$$

$$a_{i0}=\Gamma_i'(b_i^0+b_{i0}), \qquad \lambda=0.$$

Summing over all λ we have, using (3.8) and (3.9),

$$a_i=\Gamma_i'(b_i^0+b_i). \tag{3.10}$$

The analysis also preserves the familiar scattering law for the partial waves, for scattering matrix elements s_{ik}, in the form

$$b_{i\lambda}=\sum_{k\neq\lambda} s_{ik}a_{k\lambda}+s_{i\lambda}(a_\lambda^0+a_{\lambda\lambda}), \qquad \lambda\neq 0$$

$$=\sum_{k=1}^{n} s_{ik}a_{k\lambda}+s_{i\lambda}a_\lambda^0;$$

$$b_{i0}=\sum s_{ik}a_{k0}, \qquad \lambda=0.$$

Again summing over all λ we have

$$b_i=\sum_{k=1}^{n} s_{ik}(a_k^0+a_k). \tag{3.11}$$

In matrix notation (3.8), (3.9), (3.10), and (3.11) become

$$a^t=a^0+a \tag{3.12}$$

$$b^t=b^0+b \tag{3.13}$$

$$a=\Gamma' b^t \tag{3.14}$$

$$b=Sa^t, \tag{3.15}$$

where Γ' is the diagonal matrix with elements Γ_i', $i=1, 2, \ldots n$; S is the $n\times n$ scattering matrix; and the a's and b's are column matrices. These are the basic equations of the circuit and constitute the generalization of (3.3) and (3.4).

These four equations are easily solved for the matrix b_i, eliminating the unknown matrix a. We obtain, using the unit matrix 1,

$$b^t=(1-S\Gamma')^{-1}(Sa^0+b^0). \tag{3.16}$$

From the matrix form of (3.1) applied to a^t and b^t, the voltage at any port is given by

$$v=a^0+(1+\Gamma')b^t=a^0+(1+\Gamma')(1-S\Gamma')^{-1}(Sa^0+b^0). \tag{3.17}$$

This is the general solution for an n-port network. The voltage density at any port contains contributions from the terminations of all ports and from the losses within the junction itself. This shows the possibility of "leakage" from terminations other than the desired one if these terminations are not sufficiently isolated.

Now we may further generalize the situation to that of figure 3a, where scattering matrices have been introduced into each arm which will be used to perform the modulation and the balancing. We have defined the scattering matrix by (3.15). For a two-port network we may define a cascading matrix P such that

$$\begin{pmatrix} a_1 \\ b_1 \end{pmatrix} = \begin{pmatrix} p_{11} & p_{12} \\ p_{21} & p_{22} \end{pmatrix} \begin{pmatrix} b_2 \\ a_2 \end{pmatrix} \tag{3.18}$$

It is related to the scattering matrix by

$$(P) = \begin{pmatrix} p_{11} & p_{12} \\ p_{21} & p_{22} \end{pmatrix} = \begin{pmatrix} 1/s_{21} & -s_{22}/s_{21} \\ s_{11}/s_{21} & s_{12} - s_{11}s_{22}/s_{21} \end{pmatrix}. \tag{3.19}$$

This matrix has the property that the cascading matrix for a number of two-ports in series is the product of their respective cascading matrices, allowing us to deal with any combination of microwave components in each arm, even including lossy sections of line. The total cascading matrix may then be changed back into the total scattering matrix by the relation

$$\begin{pmatrix} s_{11} & s_{12} \\ s_{21} & s_{22} \end{pmatrix} = \begin{pmatrix} p_{21}/p_{11} & p_{22} - p_{12}p_{21}/p_{11} \\ 1/p_{11} & -p_{12}/p_{11} \end{pmatrix}. \tag{3.20}$$

We wish to know the equivalent source reflection coefficient Γ' and the equivalent source voltage density e' of a two-port driven by a source of reflection coefficient Γ and of voltage density e. (The index of the two-port has been temporarily suppressed.) It can easily be shown that

$$\Gamma' = s_{22} + s_{12}s_{21}\Gamma/(1 - s_{11}\Gamma). \tag{3.21}$$

One can also show that, neglecting sources within the two-port matrix,

$$e' = s_{21}(1-\Gamma)e/(1-s_{11}\Gamma)(1-\Gamma'). \tag{3.22}$$

The matrix a^0 has elements of the form of (3.5). Thus

$$a_i^0 = \tfrac{1}{2}(1-\Gamma_i')e_i' = \tfrac{1}{2}\, s_{21}^i(1-\Gamma_i)e_i/(1-s_{11}^i\Gamma_i). \tag{3.23}$$

The elements s_{21}^i are explicitly displayed since the comparison of power levels described later will depend on these elements. The matrix b^0 will depend on the properties of the junction and any source in the junction. So long as these properties are time-independent, the matrix b^0 need not be explicitly evaluated for our purposes.

Having developed this very general formalism, we now apply it to the three-port junction shown in figure 4. In this case (3.16) becomes

$$b_3^t = T_{31}a_1^0 + T_{32}a_2^0 + T_{33}a_3^0 + N_{31}b_1^0 + N_{32}b_2^0 + N_{33}b_3^0 \tag{3.24}$$

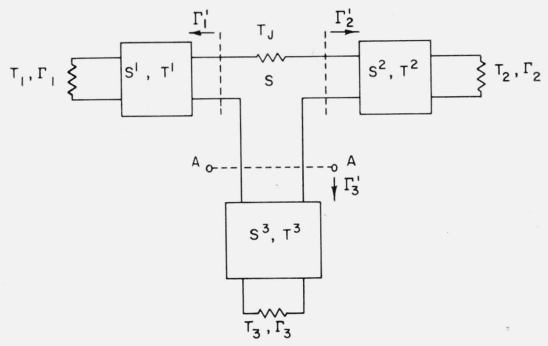

FIGURE 4. *General three-port network consisting of three equivalent scattering matrices* S^1, S^2, *and* S^3, *of temperatures* T^1, T^2, *and* T^3 *connected to a common junction characterized by a scattering matrix* S (*without superscript*) *and of temperature* T_J.

We wish to calculate the voltage at reference plane A-A.

where the coefficients are given by

$$T_{31}=N_{31}s_{11}+N_{32}s_{21}+N_{33}s_{31} \tag{3.25}$$

$$T_{32}=N_{31}s_{12}+N_{32}s_{22}+N_{33}s_{32} \tag{3.26}$$

$$T_{33}=N_{31}s_{13}+N_{32}s_{23}+N_{33}s_{33} \tag{3.27}$$

$$N_{31}=[s_{21}s_{32}\Gamma_1'\Gamma_2'+s_{31}\Gamma_1'(1-s_{22}\Gamma_2')]/\det\ (1-S\Gamma') \tag{3.28}$$

$$N_{32}=[s_{12}s_{31}\Gamma_1'\Gamma_2'+s_{32}\Gamma_2'(1-s_{11}\Gamma_1')]/\det\ (1-S\Gamma') \tag{3.29}$$

$$N_{33}=[-s_{12}s_{21}\Gamma_1'\Gamma_2'+(1-s_{11}\Gamma_1')(1-s_{22}\Gamma_2')]/\det\ (1-S\Gamma') \tag{3.30}$$

$$\begin{aligned}\det\ (1-S\Gamma')&=(1-s_{11}\Gamma_1')(1-s_{22}\Gamma_2')(1-s_{33}\Gamma_3')-s_{12}s_{23}s_{31}\Gamma_1'\Gamma_2'\Gamma_3'-s_{13}s_{21}s_{32}\Gamma_1'\Gamma_2'\Gamma_3'\\&\quad-s_{13}s_{31}\Gamma_1'\Gamma_3'(1-s_{22}\Gamma_2')-s_{23}s_{32}\Gamma_2'\Gamma_3'(1-s_{11}\Gamma_1')-s_{12}s_{21}\Gamma_1'\Gamma_2'(1-s_{33}\Gamma_3').\end{aligned} \tag{3.31}$$

We have previously noted that Γ_3' is constant. If also, through careful design and use of isolators, Γ_1' and Γ_2' are independent of changes in the quantities of (3.21) caused by modulation or substitution of different terminations Γ, all T and N coefficients in (3.25) through (3.31) are constant; and, if the b_i^0 are constant, then

$$b_3'=T_{31}a_1^0+T_{32}a_2^0+T_{33}a_3^0+\text{constant}.$$

If further a_3^0 is constant, as it would be if the elements of S^3 are constant and contain no varying sources, then

$$b_3'=T_{31}a_1^0+T_{32}a_2^0+\text{constant}. \tag{3.32}$$

For the radiometer problem, all sources in the network consist of thermal noise, so that we shall always be interested in the absolute squares of the waves, which are relatable to temperatures. Furthermore, waves arising from different thermal sources, such as a_1^0 and a_2^0 in (3.32) will be uncorrelated so that the absolute square averaged over any finite band will contain no contribution from cross products. With the understanding that this averaging will always eventually be done, such cross products will not be carried hereafter.

The spectral density of voltage for grey-body noise is [Allis and Herlin, 1952]

$$|e|^2=2kT\ \mathrm{Re}\ (z)=2kTz_0(1-|\Gamma|^2)/|1-\Gamma|^2, \tag{3.33}$$

for real z_0.[1] We use the factor $2kT$ instead of the more commonly seen factor $4kT$ because we extend the density over the axis of negative as well as positive frequency. Thus in figure 3c the absolute square launched waves are

$$|a^0|^2=\tfrac{1}{2}(1-|\Gamma_L|^2)kT_Lz_0,$$

$$|b^0|^2=\tfrac{1}{2}(1-|\Gamma_G|^2)kT_Gz_0.$$

Then in figure 3b the absolute square elements of the matrix a^0 have the form

$$|a_i^0|^2=\tfrac{1}{2}(1-|\Gamma_i'|^2)kT_i'z_0.$$

---

[1] If the characteristic impedance is complex, then z_0 in (3.33) and following work must be replaced by

$$z_0\to(\mathrm{Re}\ z_0)[1+2\ \mathrm{Im}\ z_0\ \mathrm{Im}\ \Gamma/\mathrm{Re}\ z_0(1-|\Gamma|^2)]$$

as may be verified by direct calculation of Re z in terms of Γ. The correction factor is very close to unity. If the correction is carried forward to (3.38) and (3.39), and thence to (6.1), it will almost completely cancel, except to the extent that differences in z_0 and Γ_i' for arms 1 and 2 alter the slight departure from unity of the above expression. This correction is in practice smaller than the corrections retained and is therefore dropped at this point.

If the two-ports of figure 3a are either lossless or at 0 °K, they will make no thermal contribution to e_i' or T_i' of figure 3b. The temperature T_i' equivalent to e_i' is obtained in terms of T_i and the properties of the two-port from (3.22) and (3.33). The absolute square incident waves at the reference planes of the junction are then

$$|a_i^0|^2=\tfrac{1}{2}\,|s_{21}^i|^2(1-|\Gamma_i|^2)kT_iz_0/|1-s_{11}^i\Gamma_i|^2. \tag{3.34}$$

However, when the scattering matrices are each at some temperature T^i, (3.22) must contain an additional term proportional to T^i. Equation (3.22) so modified and (3.33) give

$$|e_i'|^2=\frac{|s_{21}^i|^2|1-\Gamma_i|^2}{|1-s_{11}^i\Gamma_i|^2|1-\Gamma_i'|^2}\,2kT_iz_0\,\frac{1-|\Gamma_i|^2}{|1-\Gamma_i|^2}+A_i2kT^iz_0=2kT_i'z_0(1-|\Gamma_i'|^2)/|1-\Gamma_i'|^2 \tag{3.35}$$

where T_i is the temperature of the ith source of reflection coefficient Γ_i, T^i is the temperature of the ith scattering matrix, A_i is a coefficient to be determined, and T_i' is the temperature of the ith equivalent source of reflection coefficient Γ_i', as in figure 3b. We can evaluate the coefficient A_i by noting that, when $T_i=T^i=T_0$, we must also have by the Second Law of Thermodynamics $T_i'=T_0$. Dividing by $2kT_0z_0$ and rearranging, we obtain

$$A_i=\frac{1-|\Gamma_i'|^2}{|1-\Gamma_i'|^2}-\frac{|s_{21}^i|^2(1-|\Gamma_i|^2)}{|1-s_{11}^i\Gamma_i|^2|1-\Gamma_i'|^2}.$$

Substituting this value into (3.35) we may write

$$T_i'=\left[1-\frac{|s_{21}^i|^2(1-|\Gamma_i|^2)}{|1-s_{11}^i\Gamma_i|^2(1-|\Gamma_i'|^2)}\right]T^i+\left[\frac{|s_{21}^i|^2(1-|\Gamma_i|^2)}{|1-s_{11}^i\Gamma_i|^2(1-|\Gamma_i'|^2)}\right]T_i$$

or, equivalently,

$$(T_i'-T^i)=(T_i-T^i)\left[\frac{|s_{21}^i|^2(1-|\Gamma_i|^2)}{|1-s_{11}^i\Gamma_i|^2(1-|\Gamma_i'|^2)}\right], \tag{3.36}$$

which reduces to the former value of T_i' for $T^i=0$.

Hence in figure 3a the absolute square incident waves are in general

$$|a_i^0|^2=\tfrac{1}{2}\,kT^iz_0(1-|\Gamma_i'|^2)+\tfrac{1}{2}\,k(T_i-T^i)z_0(1-|\Gamma_i|^2)|s_{21}^i|^2/|1-s_{11}^i\Gamma_i|^2, \tag{3.37}$$

which are to be substituted into the absolute square of (3.32). The terms $\frac{1}{2}|T_{31}|^2(1-|\Gamma_1'|^2)kT^1z_0$ and $\frac{1}{2}|T_{32}|^2(1-|\Gamma_2'|^2)kT^2z_0$ are constant if Γ_1', Γ_2', T^1, and T^2 are constant.

For convenience we will absorb certain constants of proportionality into new definitions characteristic of the equivalent sources on arms 1 and 2 of figure 4:

$$|a|^2=\tfrac{1}{2}(1-|\Gamma_1|^2)k(T_1-T^1)z_0 \tag{3.38}$$

and

$$|c|^2=\tfrac{1}{2}(1-|\Gamma_2|^2)k(T_2-T^2)z_0. \tag{3.39}$$

Also, let

$$T_{31}'=T_{31}/(1-s_{11}^1\Gamma_1)$$

and

$$T_{32}'=T_{32}/(1-s_{11}^2\Gamma_2),$$

which are constant to the degree s_{11}^1 and s_{11}^2 are constant. We shall also wish to compare the temperatures of the two sources mainly in terms of the p_{11} elements of the cascading matrix defined in (3.19). Hence we define

$$p_{11}=1/s_{21}^1$$

and

$$q_{11}=1/s_{21}^2.$$

We can now write the absolute square of (3.32) as

$$|b_3^t|^2=|T'_{31}|^2\frac{|a|^2}{|p_{11}|^2}+|T'_{32}|^2\frac{|c|^2}{|q_{11}|^2}, \tag{3.40}$$

apart from an additive constant.

The important result is that, as modulation of p_{11} and q_{11} is introduced, the time dependent part of $|b_3^t|^2$ depends on the excess temperatures (T_1-T^1) and (T_2-T^2).

4. Radiometer Analysis—Receiver Portion

We now describe the transmission of $b_3^t=b_3+b_3^0$, emergent from the tee, through the mixer-IF network. Physically, we must account for the following: possible image suppression, frequency conversion of both signal and image, filtering effect of IF bandwidth, and addition of noise power by the mixer and IF. From the mathematical description of the superheterodyne process, the mixer should be considered a three-terminal-pair device, in which inputs at signal and image frequencies must be considered, as well as the output at the intermediate frequency.

We formulate the system of equations describing the mixer and IF as follows. Let e be the incident and f the emergent waves, functions of frequency; let the matrix U characterize the scattering properties; and let the arguments $\nu\pm\nu_0$ be indicated by the subscripts $\pm$, that is, $e_+=e(\nu+\nu_0)=e_+(\nu)$, $e_2=e_2(\nu)$, etc. The mixer-IF network shown in figure 5 may be described by

$$\begin{bmatrix} f_+ \\ f_- \\ f_2 \end{bmatrix}=\begin{bmatrix} u_{11} & u_{12} & u_{13} \\ u_{21} & u_{22} & u_{23} \\ u_{31} & u_{32} & u_{33} \end{bmatrix}\begin{bmatrix} e_+ \\ e_- \\ e_2 \end{bmatrix}+\begin{bmatrix} 1 & & \\ & 1 & \\ & & 1 \end{bmatrix}\begin{bmatrix} 0 \\ 0 \\ i(\nu)n(\nu) \end{bmatrix}. \tag{4.1}$$

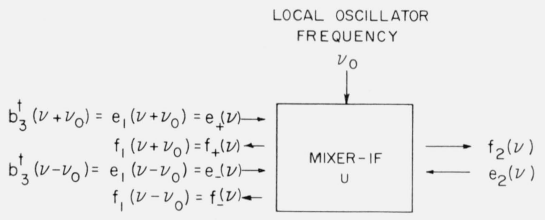

FIGURE 5. *Mixer—IF network, described by the matrix* U.

Matrix elements u_{31} and u_{32} are similarly functions of frequency, and may be written as the product of an IF amplitude response $i(\nu)$ and an RF response $r_\pm=r(\nu\pm\nu_0)=r_\pm(\nu)$. Thus $u_{31}=i(\nu)r_+$, and $u_{32}=i(\nu)r_-$. Amplitude responses are indicated by lower-case letters, and power response by capital letters, related thus: $x(\nu)x^*(\nu)=X(\nu)$, where * denotes complex conjugate. Thermal noise has been treated by considering b_3^t and a_3^t; all other noise is accounted for by the quantity n. For conventional mixers, $u_{12}=u_{13}=u_{21}=u_{23}=0$.

In the absence of any sources beyond the IF terminals we further define Γ by $e_2=\Gamma f_2$. Thus the wave emerging from the mixer-IF is

$$f_2=i(\nu)[r_+b_{3+}^t+r_-b_{3-}^t+n]/(1-\Gamma u_{33}).$$

We obtain using the rms amplitudes in (3.40)

$$f_2=\frac{i(\nu)}{1-\Gamma u_{33}}\left(\frac{T'_{31+}r_+a_+}{p_{11+}}+\frac{T'_{31-}r_-a_-}{p_{11-}}+\frac{T'_{32+}r_+c_+}{q_{11+}}+\frac{T'_{32-}r_-c_-}{q_{11-}}+n\right)+\text{constant}. \tag{4.2}$$

Using Parseval's theorem, let us average the power incident on the mixer-IF output termination over times long compared with the IF period but short compared with the modulation period by writing

$$P=z_0^{-1}\int_{-\infty}^{\infty}f_2f_2^*d\nu. \tag{4.3}$$

We note that we are concerned only with sums of absolute squares, as a_+, a_-, c_+, and c_- are all uncorrelated.

We note also that corresponding terms taken in + and − by pairs are symmetric about $\nu=0$, as are $I(\nu)$, $|1-\Gamma u_{33}|^2$, and $|n|^2$, so that the integrand as a whole is symmetric in ν, as it must be, and may be replaced by twice the integral from 0 to ∞.

We also suppose that $I(\nu)$ is relatively so narrow in the neighborhood of ν_{if} that all other quantities in the integrand may be replaced by their mean values over the band about ν_{if}.

We also choose to assume local symmetry about $\nu=\nu_0$ in the absolute squares of a, c, T'_{31}, T'_{32}, p_{11}, and q_{11}, considered individually as functions of the arguments $\nu\pm\nu_0$. Specifically, we assume at $\nu=\nu_{if}$,

$$|a(\nu_{if}\pm\nu_0)|^2=|a(-\nu_{if}\pm\nu_0)|^2.$$

Then by virtue of the symmetry of $|a|^2$ about the origin of its argument, imposed by the reality condition, namely,

$$|a(\nu+\nu_0)|^2=|a(-\nu-\nu_0)|^2,$$

we have

$$|a_+|^2=|a_-|^2\equiv a^2$$

and similarly for the other named quantities.[2]

We do not assume such local symmetry in the RF response R, in order to account for any RF frequency dependences, such as introduced by possible image suppression filters perhaps placed in arm 3 of the junction. Nevertheless, the sum R_++R_- is symmetric about $\nu=0$.

Applying these considerations to (4.3), but temporarily leaving R_++R_- under the integral, we obtain

$$P=\frac{1}{z_0|1-\Gamma u_{33}|^2}\left(\left|\frac{T'_{31}}{p_{11}}\right|^2|a|^2+\left|\frac{T'_{32}}{q_{11}}\right|^2|c|^2\right)\int_{-\infty}^{\infty}U(\nu)\,d\nu+\frac{1}{z_0|1-\Gamma u_{33}|^2}|n|^2\int_{-\infty}^{\infty}I(\nu)d\nu+\text{constant}, \quad (4.4)$$

where the quantities outside the integral are evaluated at $\nu=\nu_{if}$ and where

$$U(\nu)=[R(\nu+\nu_0)+R(\nu-\nu_0)]I(\nu). \quad (4.5)$$

We now introduce the equivalent IF bandwidth referred to the response at ν_{if},

$$\Delta\nu=\frac{1}{2I(\nu_{if})}\int_{-\infty}^{\infty}I(\nu)d\nu. \quad (4.6)$$

Finally, extracting R_++R_-, we have

$$P=\frac{2I(R_++R_-)\Delta\nu}{z_0|1-\Gamma u_{33}|^2}\left(\frac{|T'_{31}|^2|a|^2}{|p_{11}|^2}+\frac{|T'_{32}|^2|c|^2}{|q_{11}|^2}\right)+\frac{2I\Delta\nu}{z_0|1-\Gamma u_{33}|^2}|n|^2+\text{constant}, \quad (4.7)$$

where the quantities are evaluated at ν_{if}.

This is the power emergent from the IF amplifier in terms of the waves a and c leaving the two noise sources which are to be compared, and contains the effects of the waveguide attenuators and modulators and all noise.

The following illustrates the power spectrum at various points in the receiver to provide a better qualitative understanding of receiver operation. The receiver may observe an RF spectral region $U'(\nu)$, qualitatively like the rectangular pair example in figure 6. This result is available by simple and obvious changes of variables in the function $U(\nu)$ in (4.5).[3]

---

[2] If such symmetry does not exist in the spectral characteristics of a and c, then they must be treated as R immediately below. Lack of symmetry would cause errors in the radiometry unless circumvented by image suppression.

[3] In the right-hand member of (4.5), first make the change of variable $\nu'=\nu+\nu_0$ in the term $R(\nu+\nu_0)I(\nu)$, to obtain $R(\nu')I(\nu'-\nu_0)$. Then make the change $\nu''=\nu-\nu_0$ in the term $R(\nu-\nu_0)I(\nu)$ to obtain $R(\nu'')I(\nu''-\nu_0)$. Dropping the primes and adding, we obtain the new function of ν,

$$U'(\nu)=R(\nu)[I(\nu+\nu_0)+I(\nu-\nu_0)].$$

The power represented by (4.7) is slowly modulated at an audiofrequency ν_m through the time dependence of p_{11} and q_{11}. The IF amplifier is usually followed by an envelope detector. Near the origin the spectral distribution of the output of an unfiltered second detector of the quadratic, quadratic envelope, or linear envelope type is qualitatively similar to the example $Q(\nu)$ in figure 7. Quantitative results for the quadratic envelope and linear envelope detectors are given in Lawson and Uhlenbeck [1950].

An audiofrequency filter at ν_m of width $\Delta\nu_G$ selects the fundamental modulated component of the second detector output voltage, designated by subscript m, and rejects the d-c and second harmonic components. The spectral density $W(\nu)$ after the audiofrequency filter is qualitatively similar to the example shown in figure 8, where the frequency scale has been appropriately expanded.

To obtain a d-c output to drive a chart recorder, the modulation filter output may be further rectified by a third detector. Analysis may be carried through quantitatively for the case of no modulation signal, depending on the particular type of detector. For either a quadratic envelope or linear envelope detector, the spectral distribution $W'(\nu)$ is qualitatively similar to figure 9, with details available in Lawson and Uhlenbeck [1950] as to the dependence of the spike area and triangle height on $W(\nu_m)$ and B_G. If a signal at ν_m is present due to the modulation, the spike area will greatly increase; and there will also be a continuous rectangular spectrum arising from beats of signal and noise, also described in Lawson and Uhlenbeck [1950]. To further reduce output fluctuations, the extent of the spectrum may be cut off at an arbitrarily small frequency (for example less than B_G) by controlling the bandwidth of the low pass filter.

The recorder is driven by this spectrum, the area under the zero frequency component providing the mean deflection and the nonzero components contributing to the residual fluctuations. The receiver thus finally indicates that Fourier amplitude at or near ν_m (or its square if there are two square-law devices) of the time-varying power given by (4.7). Specifically, the receiver is very insensitive to the constant terms in that equation.

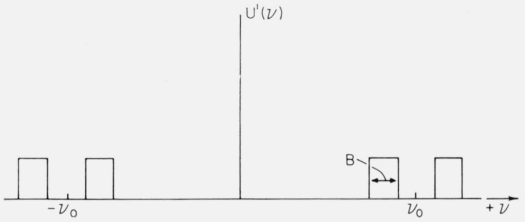

FIGURE 6. *Spectral region observed by receiver of rectangular pair response (no image suppression).*

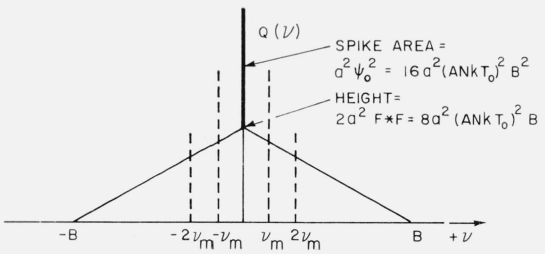

FIGURE 7. *Spectral density near the origin of output of square law second detector, fed by rectangular pair.*

If the input noise power is modulated corresponding to a temperature change ΔT, signal peaks, qualitatively shown by the dotted lines, appear at the first and second harmonic, corresponding to a signal amplitude proportional to ΔT. A large d-c component exists [Lawson and Uhlenbeck, 1950]. The d-c component and the second harmonic peaks are discriminated against by a modulation frequency filter. This avoids practical problems of the usual d-c detection such as d-c gain instabilities and could facilitate the obtaining of narrow post-detection bandwidths by synchronous detection at ν_m, for example.

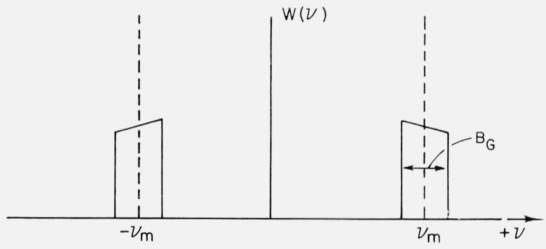

FIGURE 8. *Spectral density after the modulation frequency filter, G(ν), of rectangular response.*

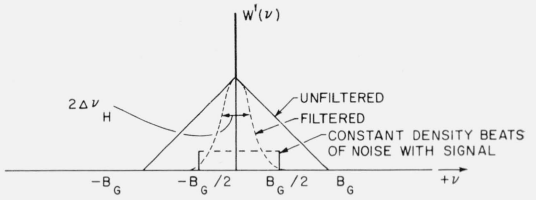

FIGURE 9. *Qualitative spectral density after a third detector fed by W(ν) of figure 8.*

The analysis is that of a CW signal in a band of noise $\Delta\nu_G$ [Lawson and Uhlenbeck, 1950]. A large d-c component exists. Results are qualitatively similar for either a square-law detector or a linear detector. The dependence of the spike area and the continuous spectra on signal and noise may be found in the reference, for both cases.

5. Radiometer Output Fluctuations

Output fluctuations should be analyzed to estimate to what extent, if any, they may limit the attainable accuracy. The general problem is that of modulated noise passing through successive stages of detection, any stage of which may consist of quadratic, linear envelope, or some other kind of detector. To get solutions for the purpose of either design evaluation or performance evaluation, the problem must be specialized to a particular configuration. Examination of many possible designs is beyond the intent of this paper; but for completeness a particularly simple example will be given, which is satisfactory for our purpose, and which is a slight extension of the usual analyses in that it discusses the modulation filter and the third detection. More refined analyses may be made using the appropriate references [Rice, 1945; Lawson and Uhlenbeck, 1950; Colvin, 1959].

At the balance condition, even though $|a_1^0|^2$ and $|a_2^0|^2$ are modulated, $|b_3'|^2$ appears unmodulated. We shall calculate the fluctuations in the absence of modulation of $|b_3'|^2$, and then compare them with a signal due only to the modulation of $|b_3'|^2$, assuming that the fluctuations do not significantly change when modulation is introduced. We shall assume that the input to the second detector is a noise amplitude, $f(t)$, having Gaussian probability density, characterized by some noise figure N which contains both the equivalent source temperature T_G which produces b_3', and noise arising within the mixer—IF. We shall assume, in figure 2b, a quadratic second detector, followed by a modulation filter and by a linear third detector. The input to the square-law second detector consists solely of a noise voltage $f(t)$ of spectral density $F(\nu)$ given by the integrand of (4.3). The autocorrelation function of this voltage,

$$\psi_\tau = \lim_{T\to\infty} \frac{1}{T}\int_0^\infty f(t)f(t+\tau)dt,$$

is related to the spectral density by

$$\psi_\tau = 2\int_0^\infty F(\nu)\ \cos\ 2\pi\nu\tau d\nu; \tag{5.1}$$

and the mean square value of the voltage is

$$\psi_0 = 2\int_0^\infty F(\nu)d\nu. \tag{5.2}$$

Rice [1945, his eq (4.10–1)] has shown that for a quadratic device [output $q(t) = af^2(t)$] the autocorrelation function of the output is given in terms of the autocorrelation function of the input by

$$\Psi(\tau) = a^2(\psi_0^2 + 2\psi_\tau^2). \tag{5.3}$$

The power spectrum is, since $\Psi(\tau) = \Psi(-\tau)$,

$$Q(\nu) = 2\int_0^\infty \Psi(\tau)\ \cos\ 2\pi\nu\tau d\tau. \tag{5.4}$$

Conversely, since $Q(\nu) = Q(-\nu)$, we have

$$\Psi(\tau) = 2\int_0^\infty Q(\nu)\ \cos\ 2\pi\nu\tau d\nu. \tag{5.5}$$

We note in passing that practical square-law detectors responding to band-limited noise about some intermediate frequency do not often have this law, as they do not respond to the second harmonic component implicit in the law. Rather, they may be more properly called quadratic envelope detectors, having output proportional to the square of the envelope of $f(t)$, that is, to the power averaged over many IF cycles. Nevertheless, it may be verified

that for band-limited noise such as from an IF amplifier, the output spectra of the quadratic detector and the quadratic envelope detector are identical except for contributions in the neighborhood of the second harmonic, which are filtered anyway. We may thus consider the analysis of the quadratic detector quite applicable.

Let $G(\nu)|$ denote the power response of the modulation filter. Then the spectral density $W(\nu)$ shown in figure 8 at the output of the modulation filter is

$$W(\nu)=G(\nu)Q(\nu). \tag{5.6}$$

Let us proceed to assemble $W(\nu)$. From (5.4), (5.3), and (5.6) we obtain, after integration,

$$W(\nu)=a^2G(\nu)[\psi_0^2\delta(\nu)+4\int_0^\infty \psi_\tau^2\cos\,2\pi\nu\tau d\tau], \tag{5.7}$$

using the representation

$$\delta(\nu)=2\int_0^\infty \cos\,2\pi\nu\tau d\tau, \tag{5.8}$$

which has the property

$$\int_{-\infty}^{\infty} A(\nu)\delta(\nu)\,d\nu=A(0). \tag{5.9}$$

The convolution theorem states that the Fourier transform of the product of two functions is the convolution of their transforms. Thus, using * to mean convolute rather than complex conjugate,

$$2\int_0^\infty \psi_\tau\psi_\tau\cos\,2\pi\nu\tau d\tau=\int_{-\infty}^{\infty} F(\nu-\nu')F(\nu')d\nu'=F^*F, \tag{5.10}$$

an even function of ν. Using this relation, (5.7) becomes

$$W(\nu)=a^2G(\nu)[\psi_0^2\delta(\nu)+2F^*F]. \tag{5.11}$$

Figures 7 and 8 show $Q(\nu)$ and $W(\nu)$ for a particular example.

We wish to find the mean square fluctuations $\overline{w^2}-\overline{w}^2$ in $w(t)$, the voltage after the modulation filter. It is obvious that

$$\overline{q}=a\psi_0$$

and

$$\overline{w}=\overline{q}g(0), \tag{5.12}$$

where $g(\nu)$ is the amplitude response of $G(\nu)$. For the case in hand, $g(0)=0$.

The mean square voltage after the modulation filter is the integral of $W(\nu)$ over all frequencies. The function F^*F, which is related to the IF amplifier response $I(\nu)$, is very slowly varying over the band of $G(\nu)$. We assume that it may be replaced by its value at ν_m and removed from under the integral sign. Hence we have

$$\overline{w^2}=a^2G(0)\psi_0^2+2a^2F^*F|_{\nu_m}\int_{-\infty}^{\infty} G(\nu)d\nu. \tag{5.13}$$

We define the equivalent width of the function $G(\nu)$ in the usual way,

$$\Delta\nu_G=\frac{1}{2G(\nu_m)}\int_{-\infty}^{\infty} G(\nu)d\nu. \tag{5.14}$$

Values of $\Delta\nu_G$ for a number of filters are given by Colvin [1959]. The mean square fluctuations after the modulation filter are then

$$\overline{\Delta w^2}=\overline{w^2}-\overline{w}^2=4a^2F^*F|_{\nu_m}G(\nu_m)\Delta\nu_G, \tag{5.15}$$

which is simply the area of the continuous spectrum illustrated by figure 8.

The function $F(\nu)$ is proportional to $I(\nu)$ by (4.4) and (4.5), since $R(\nu+\nu_0)+R(\nu-\nu_0)$ is slowly varying where $I(\nu)$ is significantly different from zero.

The form of $F(\nu)$ may then be rewritten as

$$F(\nu)=A(T_G/T_0+n)kT_0I(\nu)=ANkT_0I(\nu), \tag{5.16}$$

where A is a constant of the instrument, T_G is the equivalent temperature of the equivalent source at the receiver input terminals described in figure 3c and (3.32), and n accounts for constant noise. For the purpose at hand, it is sufficient to ascribe all this noise power density to an operating noise factor N, in the usual way, as shown. We remark parenthetically the well-known fact that N depends on T_G; and the better the noise factor, the more sensitive is the dependence. From (5.16), it is evident that

$$F^*F|_{\nu_m}=(AkNT_0)^2I^*I|_{\nu_m}.$$

Writing $\Delta w=(\overline{\Delta w^2})^{1/2}$ for simplicity, the output fluctuations are

$$\Delta w=aAkNT_0[4I^*I|_{\nu_m}G(\nu_m)\Delta\nu_G]^{1/2}.$$

Next we ask what output signal occurs when we intentionally introduce an equivalent temperature change ΔT_G at the input to the receiver. We note that F, ψ_0, and $\overline{q}$ will change by amounts $\Delta F=Ak\Delta T_GI(\nu)$, $\Delta\psi_0$, and $a\Delta\psi_0$, respectively. If this change is carried out sinusoidally at the modulation frequency, assumed slow compared to the times over which the correlation functions and spectral densities are evaluated, a signal of amplitude w_s will pass the modulation filter such that

$$w_s=a|g(\nu_m)|\Delta\psi_0=aAk\Delta T_G[G(\nu_m)]^{1/2}\int_{-\infty}^{\infty}I(\nu)d\nu.$$

This amplitude could be obtained more formally and elegantly perhaps, but surely less directly, by incorporating the effect of modulation into $\psi(\tau)$ and $Q(\nu)$; but for this purpose the simpler argument will do. Following Colvin [1959], we may obtain the equivalent width of the function I^*I as

$$\Delta\nu_{I^*I}=\frac{1}{2I^*I|_0}\int_{-\infty}^{\infty}I^*Id\nu=\frac{1}{2I^*I|_0}\left[\int_{-\infty}^{\infty}I(\nu)d\nu\right]^2, \tag{5.17}$$

using (5.16), (5.10), (5.8), (5.9), and (5.2). Values for a number of such receiver responses are given in figure 10, and are found to be closely related to the width of the IF response.

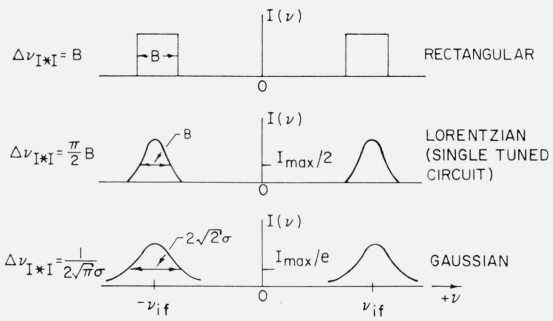

FIGURE 10. *Bandwidths for several IF responses [after Colvin, 1959].*

In terms of these quantities the ratio of rms noise fluctuations to signal amplitude is

$$\Delta w/w_s=(\sqrt{2}NT_0/\Delta T_G)(\Delta\nu_G/\Delta\nu_{I^*I})^{1/2}(I^*I|_{\nu_m}/I^*I|_0)^{1/2}. \tag{5.18}$$

The third factor is very close to unity because ν_m is close to zero compared to the IF bandwidth, and we neglect its departure from unity. For signal to fluctuation ratio of unity, we find, dropping the subscript G on ΔT_G,

$$\Delta T = \sqrt{2}(\Delta\nu_G/\Delta\nu_{I*I})^{1/2} N T_0. \tag{5.19}$$

The analysis of an unmodulated radiometer employing d-c output and low-pass post-detection smoothing filter is contained in (5.13) and (5.12) and gives the same result as (5.19). The result essentially agrees with Dicke [1946].

So far the minimum detectable ΔT depends only upon two bandwidths and the system noise figure. It depends upon signal level only as this enters into the noise factor. In the spectrum of the fluctuations, the d-c terms have been suppressed by the use of modulation and the modulation filter, so the drift is eliminated to the extent that a-c amplifiers are more stable in gain than d-c amplifiers. Furthermore, gain variations at frequencies outside the bandwidth of the modulation filter do not affect the balance. In practical instruments, narrow bandwidth at ν_m may be obtained by twin-tee circuitry, tuned feedback amplification, or synchronous detection at this point. We note in passing that due to the spectral distribution shown in figure 7 having a triangular shape, there is in principal a reduction of background noise when $\nu_m \to B$. In our case ν_m is relatively close to zero, and the effect is unimportant. In some applications sensitivity may be increased by raising the modulation frequency.

Corresponding to a minimum detectable temperature change is a minimum detectable change in available noise power given by

$$\Delta P_{\min} = k\Delta T \Delta\nu. \tag{5.20}$$

Equations (5.19) and (5.20) were used to compute the sensitivity of a receiver with a rectangular pair reception filter and an ideal low-pass smoothing filter. The computed figures agree well with experimental values, indicating that the assumptions employed in this section are reasonable.

It is not too difficult, following Lawson and Uhlenbeck [1950], to continue the analysis through the third detector and to examine the various possible combinations such as quadratic-quadratic, quadratic-linear, linear-linear, and linear-quadratic. Only qualitative results will be noted here, however. For the linear-linear and quadratic-linear combinations, the overall rms fluctuation-to-signal dependence is of the form of (5.18) except with $\Delta\nu_H$, the width of the low-pass filter, replacing $\Delta\nu_G$, and thus enabling a narrower post-detection bandwidth. For the quadratic-quadratic and linear-quadratic cases, the overall rms fluctuation to signal dependence is as

$$\frac{\Delta w'}{w_s'} \propto \left(\frac{NT_0}{\Delta T}\right)^2 \frac{(\Delta\nu_G \Delta\nu_H)^{1/2}}{\Delta\nu_{I*I}}.$$

The equivalent post-detection band is the geometric mean of the G and H filter widths. The criterion, rms fluctuation equal to signal, still gives an expression of the form of (5.19) for minimum detectable ΔT.

6. Balancing Procedures

Modulation of the elements p_{ij} and q_{ij} of the cascading matrices P and Q by any function of time produces a related time dependence of the power P in (4.7), through the two terms in which $|a|^2$ and $|c|^2$ appear. For the term in $|a|^2$ the major time dependence is in the factor $1/|p_{11}|^2$. The quantity $|T_{31}'|$ of (4.7) is slightly time dependent through s_{11}^1 (an element of the scattering matrix corresponding to the cascading matrix P) and through Γ_1' and Γ_2' which enter in T_{31}. However, the time dependence contributed by these factors may be verified to be at greatest of the second order in small quantities (that is, small scattering matrix elements or reflection coefficients). For the purposes of this work, this is assumed negligible compared to the zeroth-order time dependence of $1/|p_{11}|^2$.

In (4.7) we may then set the fundamental modulation frequency component of the power P to a minimum given by (5.19) and (5.20). The radiometer is used as in figure 11a with sources

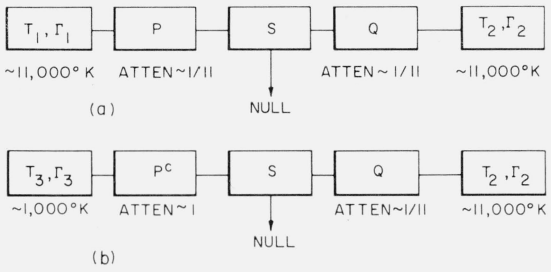

FIGURE 11. *Balancing procedure, Example A.*
Substitution of standard T_3, Γ_3 for unknown T_1, Γ_1.

T_1, Γ_1 and T_2, Γ_2 of (3.38) and (3.39) on arms 1 and 2 respectively. We take $T^1=T^2=T_0$ for the temperature of networks P and Q. We designate the fundamental of the time-dependent factors by the subscript m. If the modulation responses of P and Q are carefully assured to be opposite in phase at the fundamental modulation frequency, balance requires that

$$\left(\frac{1}{|p_{11}|^2}\right)_m \frac{|T_{31}|^2(1-|\Gamma_1|^2)(T_1-T_0)}{|1-\Gamma_1 s_{11}^1|^2}=\left(\frac{1}{|q_{11}|^2}\right)_m \frac{|T_{32}|^2(1-|\Gamma_2|^2)(T_2-T_0)}{|1-\Gamma_2 s_{11}^2|^2}. \tag{6.1}$$

We have recognized that the fundamental component of the reciprocal of a function of time is not in general equal to the reciprocal of the fundamental component of the function. Equation (6.1) is important as the balance equation of the instrument, from which measurements and errors for any method of operation may be obtained.

Example A. If we substitute a source T_3, Γ_3 of absolutely known value, here supposed to be the standard, on arm 1 as in figure 11b, and rebalance by adjusting only p_{11} to a changed value p_{11}^c, we have the new balance equation

$$\left(\frac{1}{|p_{11}^c|^2}\right)_m \frac{|T_{31}|^2(1-|\Gamma_3|^2)(T_3-T_0)}{|1-\Gamma_3 s_{11}^{1c}|^2}=\left(\frac{1}{|q_{11}|^2}\right)_m \frac{|T_{32}|^2(1-|\Gamma_2|^2)(T_2-T_0)}{|1-\Gamma_2 s_{11}^2|^2}. \tag{6.2}$$

Note that $\Gamma_1 s_{11}^1$ has gone into $\Gamma_3 s_{11}^{1c}$ because of the source interchange and the readjustment of the network P. The quantity $|T_{31}|^2$ depends on the reflection coefficient placed on arm 1, from (3.25) and (3.28) through (3.31). The dependence stems from terms only of second order and higher in small quantities (that is, reflection coefficients or small scattering matrix elements). In practice this dependence may be reduced to terms of higher order if isolators, which tend to keep Γ_1' constant although Γ_1 changes, are included in arm 1. Similar remarks apply to $|T_{32}|^2$.

The source T_2, Γ_2 serves only as a reference comparison, and its characteristics as well as the characteristics of transmission in arm 2 are eliminated between (6.1) and (6.2). We obtain for source 1 in terms of source 3,

$$(1-|\Gamma_1|^2)(T_1-T_0)=\eta_A(\lambda_c^2/\lambda^2)(1-|\Gamma_3|^2)(T_3-T_0), \tag{6.3}$$

where we have abbreviated $\lambda^2=(1/|p_{11}|^2)_m$ and

$$\eta_A=|1-\Gamma_1 s_{11}^1|^2/|1-\Gamma_3 s_{11}^{1c}|^2. \tag{6.4}$$

The error factor η_A requires knowledge of only the two additional quantities s_{11}^1 and s_{11}^{1c}, both nearly equal and easily measured. If the matching is good, η_A is very nearly unity. This is the mode of operation presently in use at the National Bureau of Standards.

As a practical point, it is worth noting that the choice of the transmission characteristics of the three-port junction may be chosen to advantage in special cases. For use as in Example A, we may choose a directional coupler rather than a hybrid tee and secure the required throttling of T_2 by the coupling factor instead of by an attenuator in network Q. This design avoids an approximate 3 db power loss of the low-temperature source in the junction and improves the sensitivity as described below. The present radiometer analysis is general enough to apply to this design also.

When only comparison of sources at high temperature ($\sim$11,000 °K) is required, sensitivity of comparison is increased by the ability to keep the attenuation ratio in network P about unity instead of throttling the high-temperature sources down to the level of the low-temperature ($\sim$1,000 °K) hot-body standard source. Then a change ΔT_1 or ΔT_2 in the sources is transmitted to the receiver unattenuated, and this quantity must be equal to or greater than the minimum detectable change given by (5.19). Otherwise only the attenuated change reaches the receiver, and correspondingly greater change at the sources is required to produce the minimum detectable change at the receiver.

Example B. The constants of the instrument, T_{31}, T_{32}, and q_{11}, may be eliminated by interchanging sources 1 and 2 in (6.1) and adjusting p_{11} to a changed value p_{11}^c for rebalance, as in figure 12, which also changes s_{11}^1 to s_{11}^{1c}. Elimination of the above constants between

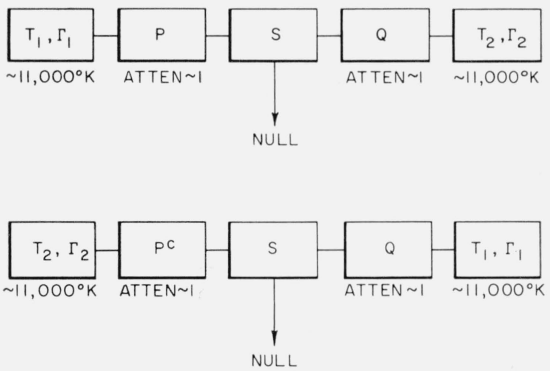

FIGURE 12. *Balancing procedure, Example B.*
Interchange of T_1, Γ_1, and T_2, Γ_2.

(6.1) and the corresponding equation describing the interchange gives for source 1 in terms of source 2,

$$(1-|\Gamma_1|^2)(T_1-T_0)=\eta_B(\lambda_c/\lambda)(1-|\Gamma_2|^2)(T_2-T_0), \tag{6.5}$$

where

$$\eta_B=|1-\Gamma_1 s_{11}^1|\,|1-\Gamma_1 s_{11}^2|/|1-\Gamma_2 s_{11}^{1c}|\,|1-\Gamma_2 s_{11}^2|. \tag{6.6}$$

Again, η_B is very close to unity for good matching. In this method, evaluation of η_B requires knowledge of the additional quantity s_{11}^2, also easily measured. This method is best used for sources of similar T, Γ. For, if the temperatures are too dissimilar, it requires excessive throttling in both arms, resulting in poor sensitivity. But the more similar the source reflection coefficients, the closer η_B becomes to unity.

Example C. An alternative method of operation may be convenient when many unknown sources are to be compared in succession with the standard, T_3, Γ_3. As a preliminary adjustment, trial sources 1 and 2 of similar T and Γ are repeatedly interchanged on arms 1 and 2, and p_{11}, q_{11}, and T_2 are adjusted until further interchange does not disturb the balance. Then in (6.1) $\lambda=\lambda_c$ and $s_{11}^1=s_{11}^{1c}$, and we may solve for the instrumental constant

$$\frac{|T_{32}|^2}{|T_{31}|^2}\left(\frac{1}{|q_{11}|^2}\right)_m=\lambda_c^2\frac{|1-\Gamma_1 s_{11}^2||1-\Gamma_2 s_{11}^2|}{|1-\Gamma_1 s_{11}^{1c}||1-\Gamma_2 s_{11}^{1c}|}. \tag{6.7}$$

The standard source T_3, Γ_3 may then be permanently installed on arm 2 as in figure 13. Then for any source T, Γ installed on arm 1 and balanced to the standard without further adjustment in arm 2, but only by adjustment of p_{11}^c to a new value p_{11} (and s_{11}^{1c} to s_{11}^1 and λ_c to λ), we have from the form of (6.5) corresponding to this situation and from (6.7),

$$(1-|\Gamma|^2)(T-T_0)=\eta_C(\lambda_c^2/\lambda^2)(1-|\Gamma_3|^2)(T_3-T_0), \tag{6.8}$$

where

$$\eta_C=\frac{|1-\Gamma_1 s_{11}^2||1-\Gamma_2 s_{11}^2|}{|1-\Gamma_1 s_{11}^{1c}||1-\Gamma_2 s_{11}^{1c}|}\frac{|1-\Gamma s_{11}^1|^2}{|1-\Gamma_3 s_{11}^2|^2}. \tag{6.9}$$

Again, η_C is very close to unity for well matched units.

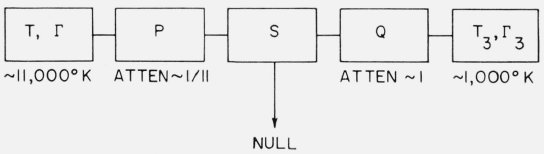

FIGURE 13. *Balancing procedure, Example C.*
Comparison of unknown T, Γ with T_3, Γ_3, having previously calibrated the instrumental constants.

These examples serve to illustrate the numerous methods of possible operation, not all of which are independent. For example, it is stated without proof that Example C reduces to Example B for T, $\Gamma=T_1$, Γ_1, and T_3, $\Gamma_3=T_2$, Γ_2. Also Example C reduces to Example A if T_3, Γ_3 replaces T, Γ in the left-hand member of (6.8) and T_2, Γ_2 replaces T_3, Γ_3 in the right-hand member.

7. Typical Error Analysis

So far we have not assumed any specific configuration for the arms of the radiometer. In order to demonstrate that a ratio such as $(1/|p_{11}^c|^2)_m/(1/|p_{11}|^2)_m=\lambda_c^2/\lambda^2$ is an attenuation ratio, and to evaluate error factors numerically, we choose a particular case where one arm consists of an attenuator and a modulator. Addition of isolators before or after this combination will not affect the result because of the properties of isolators.

We write a cascading matrix of the type defined by (3.18) for an attenuator with attenuation $|l|^2$,

$$L=\frac{1}{l}\begin{bmatrix}1 & -\Gamma_{l2}\\ \Gamma_{l1} & l^2-\Gamma_{l1}\Gamma_{l2}\end{bmatrix}, \tag{7.1}$$

where we have used the reciprocal nature of the attenuator.

We wish to write the cascading matrix M for the general case of a nonreciprocal modulator in such a way that we may easily find the fundamental component of $1/|p_{11}|^2$. The scattering matrix is

$$S_m=\begin{bmatrix}\Gamma_{m1}(t) & m_2(t)\\ m_1(t) & \Gamma_{m2}(t)\end{bmatrix}. \tag{7.2}$$

We assume the elements are constant functions of frequency over the RF pass band, and we display the slow time dependence at the modulation frequency. This time dependence in practice is, unfortunately, generally different in form and magnitude for each element. From (7.1), (7.2), and (3.19) we may form the total cascading matrix, find the element $p_{11}=(LM)_{11}$, and finally find

$$\frac{1}{p_{11}}=\frac{lm_1(t)}{1-\Gamma_{l2}\Gamma_{m1}(t)}.$$

If we take the two time dependences to be real and separable, of the form $m_1(t)=m_1 f(t)$ and $\Gamma_{m1}(t)=\Gamma_{m1}g(t)$, we see that

$$\frac{1}{|p_{11}|^2}\simeq|l|^2|m_1|^2\{[f(t)]^2+O(\Gamma^2)g(t)[f(t)]^2\},$$

where the terms through second order in small quantities (the reflection coefficients) times $g(t)$ are displayed. When the fundamental component λ^2 of each term is taken, to a very high degree of approximation,

$$\lambda_c^2/\lambda^2=|l_c|^2/|l|^2$$

because of almost complete cancellation of the second-order terms. This cancellation is the more complete the more constant Γ_{l2} is with attenuator setting. Introducing α and γ, the attenuator readings in decibels corresponding to $|l|^2$ and $|l_c|^2$, respectively,

$$|l_c|^2/|l|^2=10^{-(\gamma-\alpha)/10}. \tag{7.3}$$

Numerical evaluation of our results will permit examination of the relative importance of each source of error. First, the attenuator calibration may be certified to ± 0.01 db. Second, the error in measurement of the standard temperature T_3 may be ± 5 °K or ± 0.022 db. The output fluctuations given by (5.19) can be made negligible compared to other errors. Third, assuming the numerical magnitudes $|\Gamma|=|\Gamma_1|=|\Gamma_2|=|\Gamma_3|=0.030$, $|s_{11}^1|=|s_{11}^{1c}|=|s_{11}^2|=0.050$ (any differences may be accounted for more precisely in practice), and allowing for the most unfortunate phases, we find from (6.4), (6.6), and (6.9) that the bounds on the η's are $|\eta_A|\leq 0.026$ db, $|\eta_B|\leq 0.026$ db, and $|\eta_C|\leq 0.052$ db. If one did not know or did not wish to carry the reflection coefficients associated with each source, one could write (6.3), for example, as

$$T_1-T_0=\eta_D(\lambda_c^2/\lambda^2)(T_3-T_0), \tag{7.4}$$

where we take $\eta_D=\eta_A(1-|\Gamma_3|^2)/(1-|\Gamma_1|^2)$. If this error limit were tolerable, (7.4) could be used for the radiometer. Imperfect matching may in practice contribute significant error, so that it is evidently desirable to match the system as well as possible.

Table 1 gives a comparison of an early model (1958) NBS radiometer with a still earlier (1946) MIT radiometer and with a maser-TWT radiometer at Columbia. The measured output fluctuation of the NBS radiometer was ± 0.2 °K, which agrees roughly with (5.19). This indicates that our assumptions are in some measure reasonable.

TABLE 1. *Calculated performance of three radiometers*

Performance characteristic	MIT	NBS	Columbia [a]
Receiver noise figure	25	3.2	
IF bandwidth $\Delta\nu_{IF}$, Mc/s	8	10	5.5
Low-pass filter bw $2\pi\Delta\nu_G$, sec^{-1}	0.4	0.2	
Calculated ΔT, °K	0.95	0.08	0.02
Calculated minimum detectable power change, ergs/sec	1.0×10^{-9}	0.96×10^{-10}	0.15×10^{-10}

[a] Drake et al. [1958].

8. Summary

It is possible to derive a very general expression for the voltage wave emergent from one port of a multiport microwave junction, which itself contains sources, and to the arms of which are connected general microwave two-ports themselves terminated by active sources. This expression may be specialized to a class of microwave radiometers consisting of a three-port

junction, to the arms of which are connected, through general microwave two-ports used for measurement, respectively a microwave source to be measured, a standard source in terms of which the measurement is made, and a receiver. The analysis is sufficiently complete to identify clearly many conditions which bear on the accuracy of measurement of the unknown source, and to quantitatively evaluate them, or to keep them below some tolerable contribution.

In particular, noise arising from lossy elements anywhere in the microwave network can be explicitly taken into account. The familiar result obtains, namely that the noise associated with the excess of the source temperature over the radiometer temperature is observed; but this result is now subject to the important condition that all lossy elements of the radiometer proper be at the same temperature. Adequate isolation among arms is required to avoid contributions from arms other than the desired one. Departures from ideal impedance match in the microwave arms require corrections, which are here evaluated to second order in small quantities; this analysis constitutes the main quantitative result of the paper. For radiometers designed for rapid comparison of two sources, exactly opposite phase in the switching or modulation is necessary. Isolation against impedance changes in each arm becomes necessary for valid measurement. Correct treatment of the image response of the receiver is also necessary.

An analysis of fluctuations extends previous results for radiometers which are designed for the continuous observation of a source, and which therefore have low pass filters after the second detector. The extension applies to radiometers which are designed for rapid comparison of two sources by switching or modulation, and which therefore have band pass filters after the second detector. The sensitivity to source temperature change is dependent on the receiver noise factor, the limiting IF bandwidth, and the low frequency filter bandwidth in the same way as previously. The sensitivity of radiometers with a third detector operating on the signal at the switching or modulation frequency depends on the particular combination of linear or quadratic second and third detectors used. The spectral distribution of the fluctuations at various circuit points is useful as an aid to understanding and design.

A general balance equation for the instrument, subject to explicit simplifying conditions, may be derived and specialized to three convenient modes of operation in order to account for constants of the instrument appropriate to the two input paths. These modes are (a) substitution of a standard source for an unknown source on a particular arm, (b) interchange of a standard source and an unknown source on the two arms, and (c) calibration of the instrument so as to allow immediate comparison of an unknown source with a permanently affixed standard. Measurement is accomplished in terms of only the s_{21} (or p_{11}) element of the equivalent scattering (or cascading) matrix of the measurement arm.

Corrections to the measurement explicitly appear in terms of a relatively few pertinent reflection coefficients and scattering matrix elements. These expressions may be used either to correct the observations or to keep the errors within acceptable limits. Typically, reflection coefficient magnitudes of a few hundredths require correction of a few hundredths db. An important result is that mismatch of the standard and unknown sources to the waveguide transmission line requires correction only as the difference of the absolute squares of their reflection coefficients, and so may often reduce the severity of error if the sources are similarly mismatched.

Radiometers in use at the National Bureau of Standards, to which this analysis is applicable, have been previously described by Estin, Trembath, Wells, and Daywitt [1960], and by Wells, Daywitt, and Miller [1962].

Early work on NBS microwave noise standards was carried out by J. J. Freeman and C. R. Greenhow. Experimental work was carried out by M. M. Anderson. Acknowledgement is due W. R. Atkinson, R. W. Beatty, E. L. Crow, A. J. Estin, and J. S. Wells for their suggestions.

9. References

Allis, W. P., and M. A. Herlin, Thermodynamics and statistical mechanics, p. 198 (McGraw-Hill Book Co., Inc., New York, N.Y., 1952).

Bridges, T. J., A gas-discharge noise source for eight-millimeter waves, Proc. IRE **42,** 818 (1954).

Colvin, R. S., Faint signal limitations of radiometers, IRE WESCON pt. **8**, 52 (1959).

Dicke, R. H., The measurement of thermal radiation at microwave frequencies, Rev. Sci. Instr. **17,** 268 (1946).

Drake, F. D., and H. I. Ewen, A broad-band microwave source comparison radiometer for advanced research in radio astronomy, Proc. IRE **46,** 53 (1958).

Estin, A. J., C. L. Trembath, J. S. Wells, and W. C. Daywitt, Absolute measurement of temperatures of microwave noise sources, IRE Trans. on Instrumentation **I–9,** 209 (1960).

IRE, Standards on methods of measuring noise in linear twoports, 1959, Proc. IRE **48,** 61 (1960). IRE Subcommittee 7.9 on Noise, Representation of noise in linear twoports, Proc. IRE **48,** 69 (1960).

Johnson, H., and K. R. Deremer, Gaseous discharge super-high-frequency noise sources, Proc. IRE **39,** 908 (1951).

Knol, K. S., Determination of the electron temperature in gas discharges by noise measurements, Philips Res. Rep. **6,** 288 (1951).

Knol, K. S., A thermal noise standard for microwaves, Philips Res. Rep. **12,** 123 (1957).

Lawson, J. L., and G. E. Uhlenbeck, Threshold signals, M.I.T. Rad. Lab. Ser. No. 24, p. 62–63 (McGraw-Hill Book Co., Inc., New York, N.Y., 1950).

Mayer, C. H., T. P. McCullough, and R. M. Sloanaker, Measurement of planetary radiation at centimeter wavelengths, Proc. IRE **46,** 260 (1958).

Mumford, W. W., A broad-band microwave noise source, Bell System Tech. J. **28,** 608 (1949).

Rice, S. O., Mathematical analysis of random noise, Bell System Tech. J. **23,** 282 (1944); **24,** 46 (1945).

Selove, W., A dc comparison radiometer, Rev. Sci. Instr. **25,** 120 (1954).

Sutcliffe, H., Noise measurements in the 3-cm waveband using a hot source, Proc. Inst. Elec. Engrs. (London) **103B,** 673 (1956).

Wells, J. S., W. C. Daywitt, and C. K. S. Miller, Measurement of effective temperatures of microwave noise sources, IRE Convention Record **3,** 220 (March 1962).

(Paper 67C2–127)